REPORT DOCUMENTATION PAGE

Form Approved
OMB No. 0704-0188

1. AGENCY USE ONLY *(LEAVE BLANK)*	2. REPORT DATE	3. REPORT TYPE AND DATES COVERED
	3 February 1999	Professional Paper

4. TITLE AND SUBTITLE

Thermographic Modeling of Water Entrapment

5. FUNDING NUMBERS

6. AUTHOR(S)

Ignacio Perez William Davis Paul Kulowitch
Fred Dersha

7. PERFORMING ORGANIZATION NAME(S) AND ADDRESS(ES)

Naval Air Warfare Center Aircraft Division
22347 Cedar Point Road, Unit #6
Patuxent River, Maryland 20670-1161

8. PERFORMING ORGANIZATION REPORT NUMBER

9. SPONSORING/MONITORING AGENCY NAME(S) AND ADDRESS(ES)

Naval Air Systems Command
47123 Buse Road, Unit IPT
Patuxent River, Maryland 20670-1547

10. SPONSORING/MONITORING AGENCY REPORT NUMBER

11. SUPPLEMENTARY NOTES

12a. DISTRIBUTION/AVAILABILITY STATEMENT

Approved for public release; distribution is unlimited.

12b. DISTRIBUTION CODE

13. ABSTRACT *(Maximum 200 words)*

A common problem found in advance structural materials is water entrapment. This problem is a major cause of material degradation. In metals it can lead to corrosion and in composites it adds unnecessary weight to the structure and can lead to material degradation especially after freezing and thawing. Thermography has been investigated as a means of detecting water entrapment in metallic structures. A simple model has been derived that accurately describes the thermal response of these structures to short heat pulses. In this paper results on Aluminum panels with various amounts of water entrapment will be presented. Sensitivity relations will be derived and validated.

14. SUBJECT TERMS

NDE Thermography Thermal models Calorimetric models
Defects Water entrapment

15. NUMBER OF PAGES

8

16. PRICE CODE

17. SECURITY CLASSIFICATION OF REPORT	18. SECURITY CLASSIFICATION OF THIS PAGE	19. SECURITY CLASSIFICATION OF ABSTRACT	20. LIMITATION OF ABSTRACT
Unclassified	Unclassified	Unclassified	UL

Proceedings of SPIE, "Thermosense XXI", (J.R. Snell, R.N. Wurzbach, eds.)

Thermographic modeling of water entrapment

Ignacio Perez, William R. Davis, Paul Kulowitch
Naval Air Warfare Center, Materials Division
Patuxent River MD, 20670

Fred Dersha
Naval Surface Warfare Center, Materials Division
Carderock, MD

ABSTRACT

A common problem found in advance structural materials is water entrapment. This problem is a major cause of material degradation. In metals it can lead to corrosion and in composites it adds unnecessary weight to the structure and can lead to material degradation especially after freezing and thawing. Thermography has been investigated as a means of detecting water entrapment in metallic structures. A simple model has been derived that accurately describes the thermal response of these structures to short heat pulses. In this paper results on Aluminum panels with various amounts of water entrapment will be presented. Sensitivity relations will be derived and validated.

Keywords: NDE, thermography, thermal models, calorimetric models, defects, water entrapment

1. INTRODUCTION

The detection of entrapped water behind metallic structures is a difficult problem to solve in a nondestructive manner. X-ray radiography is commonly used to detect the entrapped water but the technique is not very portable in general and requires special safety precautions. Ultrasonic attenuation methods have been successfully used but suffer from a lack of lateral resolution. In this paper experimental thermographic results and simple thermographic models will be presented and discussed.

Simple thermographic models have been previously introduced [1,2] to successfully model the surface temperature evolution of panels with flat bottom holes. In those papers the hole diameter and depth were varied to simulate different amounts of mass loss due to corrosion. In all cases those simple thermographic models sufficed to accurately predict the maximum contrast temperatures observed in the experiments. This paper will closely follow the format and spirit of the previous references. Once again it will be seen that simple physical arguments go a long way in describing complicated thermal phenomena.

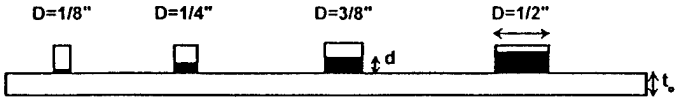

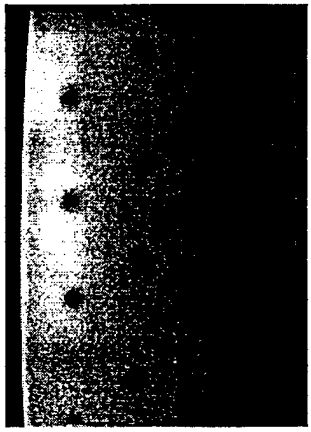

Fig. 1: (top) Drawing indicating key parameters used in study. Straws of various diameters (ranging from D = 1/8" to 1/2") were glued to aluminum panels of different thickness "t_o". The straws were filled with various amounts of water "d". (Right) Shows a single thermographic frame some time after a heat pulse. The dark regions in the image represent cold spots due to the presence of water in the back of the panel.

Experimental Parameters for Drops and Panels		
Al Thickness	Straw Diameter	Water Height
t_o = 1/32"	D = 1/8"	d = 0"
t_o = 1/16"	D = 1/4"	d = 1/16"
t_o = 1/8"	D = 3/8"	d = 1/8"
	D = 1/2"	d = 3/16"
		d = 1/4"

Table 1: This table shows the range of parameters used in this study

In this paper a simple theoretical model that contains all the relevant parameters required to describe the thermal transient process of aluminum panels with water entrapment will be presented. Some of the parameters used in the model include the amount of entrapped water, the diameter of the region with entrapped water, lateral heat flow effects, anisotropic properties, finite thickness effects of the metal plate and of the water column. In spite of the simplicity of the model, it will be seen that the model fits the experimental data remarkably well.

2. EXPERIMENTAL METHOD

The panels used in this study were imaged using a commercial pulsed IR NDT system (EchoTherm®, Thermal Wave Imaging, Inc.). Flash heating was provided by 2 linear xenon flashtubes with 5 msec flash duration, each powered by a 6.4 kJoule capacitor bank. The system was equipped with a 256 x 256 pixel InSb focal plane array camera (Radiance HS, Raytheon Amber) operating in the 2-5 micron spectral range. Continuous 12-bit data was acquired at a 120 Hz frame rate for 6 seconds after flash heating.

The material used in this study was aluminum 7075-T6. To model water entrapment, straws of different diameter were glued to the back of the panel and filled with water to various heights. Fig. 1 (Left) shows a drawing with some of the key parameters used in the model. The parameters "t_o", "D" and "d" represent the thickness of the panel, the diameter of the straws and the height of water added to the straws respectively. Three different thicknesses were chosen for the aluminum panels. Four different straw diameters were studied. The straws were filled with water to different heights. A total of 36 (3x3x4) different conditions were studied. Table 1 summarizes all the parameters used in fabricating these panels. The front side of the panels were painted with a flat black paint to avoid emissivity variation problems.

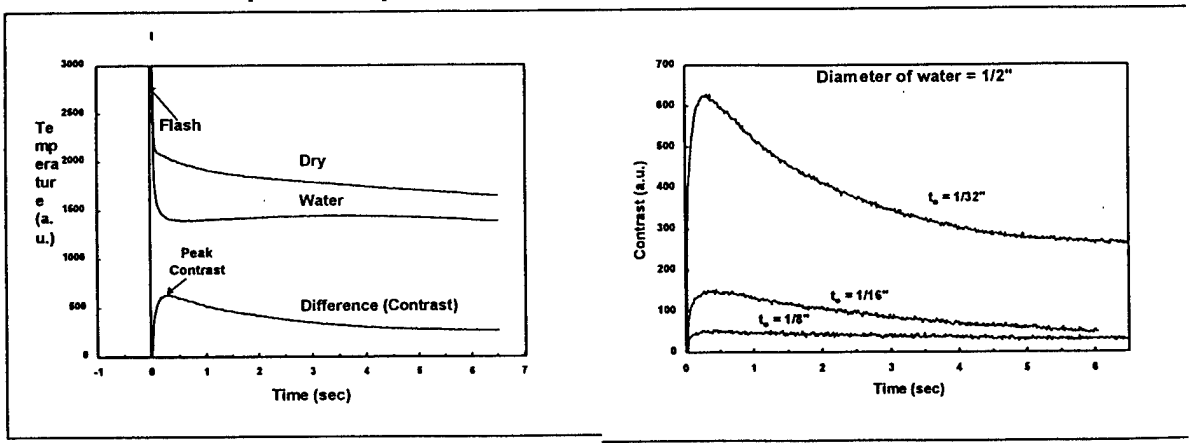

Fig. 2: (Left) This fig. shows the data curves require to generate a single contrast curve. The curve labeled "Water" represents the thermal time history of a point on the surface of the aluminum panel directly beneath a straw with filled with water. The curve labeled "Dry" represents the thermal time history of a point away from any water. The contrast curve was generated by subtracting the previous two curves. (Right) This figure shows three contrast curves for three identical water drops but for three different aluminum plate thickness.

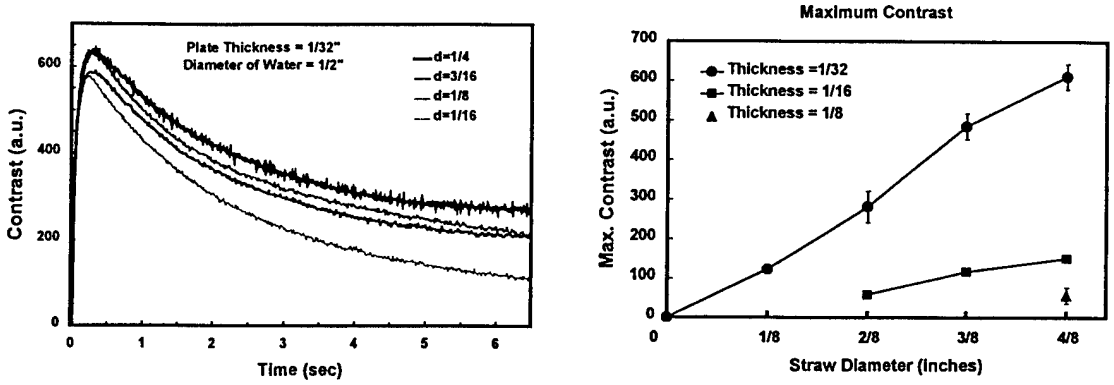

Fig. 3: (Left) This fig. shows four contrast curves for a given aluminum plate thickness and straw diameter but for four different water heights. (Right) This fig. shows the relation between the "maximum temperature contrast" for three aluminum plate thicknesses and four straw diameters.

Fig. 1 (Right) shows an actual frame taken soon after the thermal flash was shot. The dark areas in that photo indicate the presence of water in the back side of the panel. The straws were staggered so as to keep the water as far as possible from one another in order to minimize interaction effects while maximizing the number straws in one panel.

3. EXPERIMENTAL RESULTS

In a standard experiment, digital data acquisition begins a few frames before the capacitor banks are discharged through the Xenon arc lamps. In our experiments the frame rate was set to 100 frames/sec. A total of 660 frames were acquired and the entire experiment lasted over 6.6 sec. Fig. 2 (Left) shows the entire thermal history of two points on the surface of the panel. The curve labeled "water" was taken from a point directly below and in the center of a straw containing some amount of water. This curve characterizes the thermal evolution a typical site that has some water over it. The curve labeled "dry" was taken from a point far away from any straw containing water and characterizes the thermal history of a dry aluminum block. Notice that the thermal history curve labeled "water" decays faster and to a lower value than the thermal history curve labeled "dry". This is due to the fact that the "water" acts like a thermal sink, thereby producing a decrease in the surface temperature. Also notice that the "water" curve and the "dry" curve have a region at early times with very elevated effective temperature. This region of the plot is difficult to model because it includes two effects. The first effect is the direct radiation from the rapid temperature rise in the surface of the test panel due to the initial flash. The second effect is the reflected radiation from the walls of the shroud into the camera. This effects disappears when calculating the contrast curve.

The difference of the "water" curve from the "dry" curve is termed the "thermal contrast" curve (shown in Fig. 2 Left). Thermal contrast curves start and end with zero temperature since the initial surface temperature and final equilibrium temperatures are uniform throughout the entire panel. Fig. 2 (Right) shows three contrast curves for three identical water drops behind three different plate thicknesses. It is clear from that figure that the thicker the aluminum plate is the smaller the peak thermal contrast. Fig. 3 (Left) shows four contrast curves for four water drops behind a 1/32" thick aluminum panel. The diameter

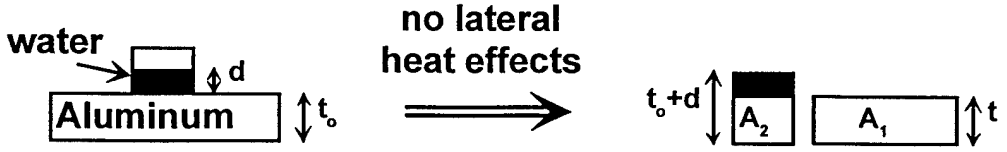

Fig. 4: This Fig. shows a schematic representation of the zero lateral flow assumption used in the model.

of the straws was kept constant an equal to ½" while the amount of water was increased. All four curves are very similar in shape and the maximum contrast value. When the experiment was repeated but with thicker aluminum plate, the four contrast curves were very similar again. These results suggest that there is some form of saturation effect when the parameters used for the experiments lay in the range as shown in Table 2. It is important to note that an ideal contrast curve is impossible to achieve since it requires two points on the surface of the panel infinitely apart. Even in a more practical sense it is very difficult to generate systematic contrast curves, because of difficulties in selecting equivalent reference point on the surface of the panel. Some of the differences seen in Fig. 3 (Left) are simply the result of difficulties in finding equivalent points over all areas of interest.

Finally Fig. 3 (Right) shows a plot of the maximum thermal contrast as a function of the straw diameter for three aluminum plate thickness. In all cases studied the effect of water content (or water height in this case) was negligible. Each data point on this graph is the average to the peak contrast for the four water contents studied (d=1/16", 1/8", 3/16" and 1/4"). The error bars represent two standard deviations of all peak contrast. In some case the standard deviations are smaller than the spot used to represent the data point. This again illustrates the fact that for the range of parameters used in this study, the effect of water height was insignificant. We will see later on how our simple model is able to account for this effect. The larger the panel thickness the smaller the contrast. For the thickest aluminum panel (t_o=1/8") only one data point could be obtained due to the small value of the maximum contrast. For the panel with thickness of 1/16" three data points were obtained.

4. CALORIMETRIC MODEL (ZEROTH ORDER APPROXIMATION)

A simple theoretical model (zeroth order approximation) has been derived and it's based on simple calorimetric arguments. Wet and dry regions are defined in this model and it is assumed that no energy flows between them. Fig. 4 shows a schematic representation of the model, where the two regions (dry and wet) have been physically separated to stress that there is no energy flow between them. In the next section a more refined model will be derived that takes into account lateral heat transfer effects.

By using simple calorimetric arguments we can write that $q_1 = \rho_1(A_1 t_o)c_1 T_1$ and $q_2 = \rho_1(A_2 t_o)c_1 T_2 + \rho_2(A_2 d)c_2 T_2$. The parameters q_1, A_1, t_o, ρ_1, and c_1 represent the energy deposited over the area A_1 of an Aluminum panel with thickness t_o density ρ_1 and the specific heat c_1. The parameters q_2, A_2, d, ρ_2, and c_2 represent the energy deposited over the area A_2 of a composite panel made from an aluminum panel of thickness t_o and a layer of water of thickness d, water density ρ_2 and the water specific heat c_2. It was assumed in this model that the initial temperature of the coupon was uniform and equal to zero degrees. Finally, if it is assumed that the energy deposited on the surface of the sample per unit area is constant, i.e., $q_1/A_1 = q_2/A_2 = Q$, then the temperature difference (or thermal contrast) between both blocks $T_1 - T_2 = \Delta T$ will be

$$\Delta T = \frac{Q}{\rho_1 c_1}\frac{1}{t_o}\left(\frac{\rho_2 c_2 \cdot d}{\rho_2 c_2 \cdot d + \rho_1 c_1 \cdot t_o}\right) \qquad (1)$$

This equation correctly describes some of the features of pulsed thermography when applied to this problem.

1. The contrast (ΔT) increases linearly with the amount of energy deposited (Q).
2. The higher the specific heat-density of the substrate ($\rho_1 c_1 \uparrow$) the smaller the peak contrast ($\Delta T \downarrow$)
3. As the water content decreases ($d \to 0$) the contrast vanishes ($\Delta T \to 0$).
4. As the amount of water grows indefinitely ($d \to \infty$) the contrast saturates ($\Delta T \to Q/\rho_1 c_1 t_o$).

It is interesting to note that this simple formula shows a strong dependence of the contrast temperature ΔT on the amount of water "d" inside the straw. As was indicated repeatedly in the previous section, this was not an experimentally observed fact. It is anticipated the lateral heat conduction effect (not included in

this model) is responsible for the insensitivity of the contrast temperature ΔT on the variable "d". In the next section a simple model that takes into account lateral heat flow effects will be presented.

5. CALORIMETRIC MODEL (FIRST ORDER APPROXIMATION)

In this section the previous model will be modified to allow for lateral heat flow effects. A "poor man's finite element approximation" (i.e. three elements only) will be used. All the elements will be thermally interconnected. Fig. 5 shows a schematic representation of this model. In this model it will be assumed that the in-plane thermal conductivity and the out-of-plane thermal conductivity are different. This will produce the most general results.

In this model it will also be assumed that all the energy of the heat pulse is absorbed the aluminum plate of thickness "t_o". As a result of this heating process, the temperature "T_o" of the aluminum plate can be derived from $Q = \rho_1 \cdot c_1 \cdot p \cdot T_o$ where it is assumed that the initial temperature of the panel was zero. The quantity K_L represents the lateral thermal conductance while K_{eff} represents the effective out of plane contact thermal conductance. The lateral thermal conductance can be expressed in terms of the lateral thermal conductivity of aluminum k_l (which in this case, since aluminum is isotropic, is just the thermal conductivity of aluminum)

$$\begin{aligned} K_L &= k_1 \cdot A_t / R \\ K_{eff} &= h \cdot A_2 \end{aligned} \tag{2}$$

Similarly, the contact conductance can be expressed in terms of an effective contact conductivity "h" between Aluminum and water. A_1 and A_2 are shown in the fig. 5 and represent the surface area of the dry region and the wet region respectively. A_2 can be written as $A_2 = \pi R^2$ where R is the radius of the straw while A_1 will be assumed to tend to infinity ($A_1 \rightarrow \infty$). A_t is not shown explicitly in the figure but represents the lateral cross sectional area and can be expressed as $A_t = 2\pi R \cdot t_o$. The set of differential equations that define this problem is

$$\begin{aligned} \rho_1 \cdot A_1 \cdot t_o \cdot c_1 \cdot \frac{dT_1}{dt} &= k_1 \cdot \frac{A_t}{R}(T_2 - T_1) \\ \rho_1 \cdot A_2 \cdot t_o \cdot c_1 \cdot \frac{dT_2}{dt} &= k_1 \cdot \frac{A_t}{R}(T_1 - T_2) + h \cdot A_2 \cdot (T_2' - T_2) \\ \rho_2 \cdot A_2 \cdot d \cdot c_2 \cdot \frac{dT_2'}{dt} &= h \cdot A_2 (T_2 - T_2') \end{aligned} \tag{3}$$

Where T_1, T_2, and T_2' are the temperatures of the different blocks as shown in Fig. 5. This set of coupled differential equations can be written in matrix form as

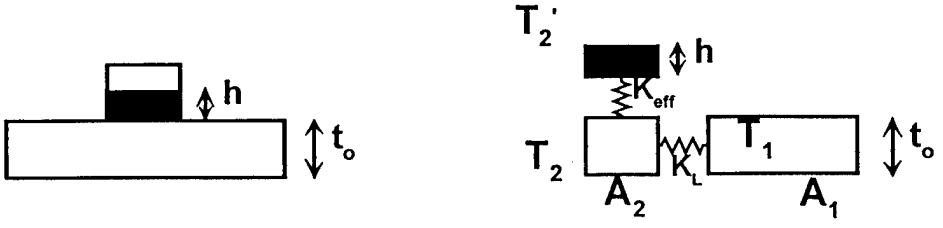

Fig. 5: This figure shows the building blocks of our simple model.

$$\begin{pmatrix} \frac{dT_1}{dt} \\ \frac{dT_2}{dt} \\ \frac{dT_2'}{dt} \end{pmatrix} = \frac{h}{\rho_1 c_1}\frac{1}{t_o}\begin{pmatrix} -\frac{k_1}{h}\frac{A_t}{A_1}\frac{1}{R} & \frac{k_1}{h}\frac{A_t}{A_1}\frac{1}{R} & 0 \\ \frac{k_1}{h}\frac{A_t}{A_2}\frac{1}{R} & -\frac{k_1}{h}\frac{A_t}{A_2}\frac{1}{R}-1 & 1 \\ 0 & \frac{\rho_1 c_1}{\rho_2 c_2}\frac{t_o}{d} & -\frac{\rho_1 c_1}{\rho_2 c_2}\frac{t_o}{d} \end{pmatrix}\begin{pmatrix} T_1 \\ T_2 \\ T_2' \end{pmatrix} \tag{4}$$

or

$$\frac{d\vec{T}}{dt} = \kappa \cdot \overline{\overline{R}} \cdot \vec{T} \tag{5}$$

This set of three coupled linear differential equations can be solved by first diagonalizing the matrix $\overline{\overline{R}}$. The second step is to transform the problem into the eigen-space where the equations get de-coupled. In this space the solutions are simple decaying exponential functions, the exponent being related to the eigen-values of the matrix $\overline{\overline{R}}$. Finally the solution in the eigen-space has to be transformed back into the original coordinate set. After performing the previous steps and imposing the following boundary conditions

$$T(t=0) = \begin{pmatrix} T_o \\ T_o \\ 0 \end{pmatrix} \tag{6}$$

where T_o is the initial temperature of the aluminum block (which can be derived from $Q = \rho_1 \cdot c_1 \cdot p \cdot T_o$) the solutions can be obtained and the contrast yields

$$\Delta T(t) = \frac{Q}{\rho_1 c_1 \cdot t_o \cdot \sqrt{(1+a+r)^2 - 4ar}}\left(e^{\frac{h}{\rho_1 c_1}\frac{\lambda_1}{t_o}t} - e^{\frac{h}{\rho_1 c_1}\frac{\lambda_2}{t_o}t} \right) \tag{7}$$

where $a = \frac{k_L}{h}\frac{A_t}{A_2}\frac{1}{R}$ and $r = \frac{\rho_1 c_1}{\rho_2 c_2}\frac{t_o}{d}$ (don't confuse the variable "t = time" with the parameter "t_o = panel thickness"). The parameters λ_1 and λ_2 are the non-trivial eigen-values of the matrix $\overline{\overline{R}}$ defined above.

The maximum or peak thermal contrast can be calculated by differentiating Eq. 7 and the result gives

$$\Delta T_{peak} = \frac{Q}{\rho_1 c_1}\frac{2}{t_o(1+a+r+\sqrt{(1+a+r)^2-4ar})} \cdot \left[\frac{1+a+r-\sqrt{(1+a+r)^2-4ar}}{1+a+r+\sqrt{(1+a+r)^2-4ar}} \right]^{\frac{1+a+r-\sqrt{(1+a+r)^2-4ar}}{2\sqrt{(1+a+r)^2-4ar}}} \tag{8}$$

which happens at a time give by

$$t_{peak} = \frac{\rho_1 c_1}{h}\frac{t_o}{\sqrt{(1+a+r)^2-4ar}} \ln\left(\frac{1+a+r+\sqrt{(1+a+r)^2-4ar}}{1+a+r-\sqrt{(1+a+r)^2-4ar}} \right) \tag{9}$$

It can be shown that in the limit when the lateral heat flow effects disappear, i.e $k_L \rightarrow 0$ (or $a \rightarrow 0$) then Eq. 8 reduces to Eq. 1 as it would be expected. In practice the contact conductivity "h" is much smaller that

the lateral thermal conductivity of aluminum "k_l", as a result a >> r > 1. If eqs. 7, 8 and 9 are expanded around "a" in this limit, it can be shown that

$$\Delta T(t) = \frac{Q}{\rho_l c_l \cdot t_o \cdot a}\left(e^{-\frac{h}{\rho_2 c_2 d} t} - e^{-\frac{k_l}{\rho_l c_l R^2} t} \right) \tag{10}$$

$$\Delta T_{peak} = \frac{Q}{\rho_l c_l} \frac{1}{a \cdot t_o} \cdot \left[\frac{r}{a} \right]^{\frac{r}{a}} \tag{11}$$

and finally

$$t_{peak} = \frac{\rho_l c_l}{h} \frac{t_o}{a} \ln\left(\frac{a}{r} \right) \tag{12}$$

It is important to stress that the previous three equations were derived in the limit a >> r, which happens to be the "material parameter space" region considered in this work as shown in Table 1. As an example, a vanishing amount of water in a straw, i.e. when d << t_o, would not fall within these "material parameter space" region and therefore would not be properly modeled by the previous equations. A desirable property of eq. 11 is that it depends very weakly on the variable "d". This weak dependence on "d" was experimentally observed and was described in section 3. The variable "d" only enters into eq. 11 via the parameter "r". If "r" << "a" then $(r/a)^{r/a} \rightarrow 1$ and ΔT actually becomes an independent function of "d".

6. ANALYSIS OF RESULTS

Figure 6 (left) shows all experimental data points and the fit to them using eq. 11. It can be seen from the graph that this simple model fits the experimental results fairly well. The largest fitting discrepancies happen for the panel with thickness 1/32". Figure 6 (right) shows the ½" straw diameter data curves for three different panel thickness and a fit to them using eq. 13. It can be seen again that the fitting results for the 1/32" thick panel show the largest discrepancies. The starting parameters that were used for all these fits are shown in table 1 and were obtain from standard material properties handbooks except for the contact conductivity. The final fitting values were found to be reasonably close to these starting parameters. The starting value for the contact conductivity was chosen to be the thermal conductivity of water per unit centimeter. The final fitting value was found to be significantly larger than this initial estimate.

Aluminum 7075 T6	Water
$\rho_1 = 2.8$ g/cm^3	$\rho_2 = 1$ g/cm^3
$c_2 = 0.84$ J/(g K)	$c_2 = 4.1$ J/(g K)
$k_l = 1.29$ W/(cm K)	$h = 8.2$ mW/(cm^2 K)

Table 2: Relevant material property values

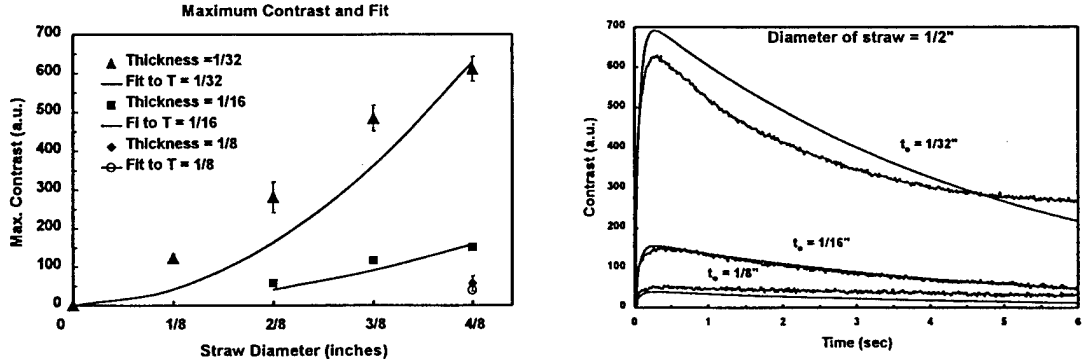

Fig. 6: This figure shows a fit (solid lines) using eqs. 8 or 11 to the experimental contrast data for three different plate thicknesses. The error bars represent the range in peak contrast temperatures for the various amounts of water used in the experiments.

It is important to emphasize some of the problems found when dealing with the type of data described in this paper and when using this simple model. The first problem that one is faced with is in generating the contrast curves. As was mentioned in section three, and ideal contrast curve should be generated by subtracting a reference curve taken far away from any region of the panel that has water from a curve taken under a region with water. This requirement was difficult to meet because of the finite size of our sample and because of the many regions with water that we had in our panel. To overcome this difficulty one could use one aluminum panel for each water drop geometry. The problem with this approach would be that a large number of panels would be require and non-systematic errors would be introduced to the data such as room temperature variations and varying amounts of heat deposited onto the surface of the sample. Another source of random errors was the straw fabrication. Straws were not perfectly circular and the diameter as a result had random errors.

The model used in this work makes some drastic approximations such as; 1) a very small number of blocks with average temperatures to describe the transient behavior of the system, 2) temperature independent material properties, 3) no cooling effects introduced through radiation, 4) uniform initial temperature distribution, 5) single drop on panel (as opposed the multitude of drops actually used in the panels), 6) transverse conductivity approximated by a contact conductance and 7) does not take into account the thermal properties of the straw. It is anticipated that many refinements to the model can be achieved by improving on some of the approximations. Despite its crudeness the model is robust enough to fit the experimental data accurately enough.

7. CONCLUSION

Two simple models have been developed (figs. 4 and 5) that to a first order approximation describes the main features of thermal pulse analysis when applied to a planar flaw. The first model, zeroth order approximation does not take into account lateral heat conduction effects. The second model takes into account lateral heat conduction effects, thickness effects, water size effects, density effects, thermal transients. The model correctly predicts the relationships between the previous parameters. Eqs. 7, 8 and 9 are the main output of the mode or their expansions around he parameter "a" (eqs. 10, 11 and 12) . This relations were shown to model correctly the time dependence of the thermal contrast, the peak thermal contrast and the time at which the thermal contrast peaks.

8. ACKNOWLEDGEMENTS

This work was supported by Mr. Jim Kelly from the Office of Naval Research by Work Request under document number N0001498WX20360.

9. REFERENCES

1 I. Perez, P. Kulowitch and S. Shepard, "Modeling of pulsed thermography in anisotropic media". Proceedings of the 25th Annual Progress in QNDE, Snowbird Colrado, July 19-24, 1998

2 I. Perez, R. Santos, P. Kulowitch and M. Ryan. "Calorimetric Modeling of thermographic data". Thermosense XX,